

CrossPyramid: Neural Ordinary Differential Equations Architecture for Partially-observed Time-series

Futoon M. Abushaqra^{1*}, Hao Xue², Yongli Ren¹ and Flora D. Salim²

¹School of Computer Science and Information Technology, RMIT University, 124 La Trobe St, Melbourne, 3000, Victoria, Australia.

²School of Computer Science and Engineering, University of New South Wales (UNSW), Computer Science Building (K17), Engineering Rd, Sydney, 2052, NSW, Australia.

*Corresponding author(s). E-mail(s):
s3803592@student.rmit.edu.au;

Contributing authors: hao.xue1@unsw.edu.au;
yongli.ren@rmit.edu.au; flora.salim@unsw.edu.au;

Abstract

Ordinary Differential Equations (ODE)-based models have become popular foundation models to solve many time-series problems. Combining neural ODEs with traditional RNN models has provided the best representation for irregular time series. However, ODE-based models require the trajectory of hidden states to be defined based on the initial observed value or the last available observation. This fact raises questions about how long the generated hidden state is sufficient and whether it is effective when long sequences are used instead of the typically used shorter sequences. In this article, we introduce CrossPyramid, a novel ODE-based model that aims to enhance the generalizability of sequences representation. CrossPyramid does not rely only on the hidden state from the last observed value; it also considers ODE latent representations learned from other samples. The main idea of our proposed model is to define the hidden state for the unobserved values based on the non-linear correlation between samples. Accordingly, CrossPyramid is built with three distinctive parts: (1) ODE Auto-Encoder to learn the best data representation.

(2) Pyramidal attention method to categorize the learned representations (hidden state) based on the relationship characteristics between samples. (3) Cross-level ODE-RNN to integrate the previously learned information and provide the final latent state for each sample. Through extensive experiments on partially-observed synthetic and real-world datasets, we show that the proposed architecture can effectively model the long gaps in intermittent series and outperforms state-of-the-art approaches. The results show an average improvement of 10% on univariate and multivariate datasets for both forecasting and classification tasks.

Keywords: Irregular time series, ODE-based models, Attention, Partially-observed time series

1 Introduction

Time series analysis of a complex irregular system is regarded as one of the contemporary data science big problems [1]. Irregular time series capture dynamic observations without a constant time basis, making them hard to be modeled [2]. Over the last few years, traditional techniques have been used to address this issue (e.g. imputation and aggregation) [3–6]. However, these methods change the structure and the temporal dependencies of the data; therefore, they were not considered real solutions. Recently with the advance of Neural Ordinary Differential Equations (Neural ODEs) [7] that can produce networks with continuous hidden states, handling irregular sequences became possible. Where traditional RNN shows a weak performance when applying it to irregular data [8], combining it with ODEs Neural Network and taking advantage of the ODEs’ ability to provide a continuous hidden state has achieved state-of-the-art results.

Recent models like ODE-RNN, Latent-ODE [9], and GRU-ODE [10] are the most popular architectures to process irregular time series. However, ODE describes the evolution in time of a process that depends on one variable (initial condition) [7]. Therefore, for the ODE-based models, the continuous trajectories of the hidden state are described by one variable (either the initial value or the last observed value). Since this trajectory represents the data, it is important to have the best-hidden representation possible. ODEs are effective but may not provide the optimal representation for the whole sequence, especially when using sequences with long time lapses between observations and partially-observed time series (e.g. medical reports data). In such cases, the hidden states count on one initial value for a long time.

In this work, we present a novel ODE-based architecture that does not rely on one trajectory to represent the data; it also produces more generalized hidden trajectories. Our architecture consists of three major parts; (1) an ODE Auto-Encoder (AE), inspired by the traditional Denoising AE [11]; this part is used to generate the best learned hidden trajectories, (2) a pyramidal attention module that categorizes the learned trajectories based on the

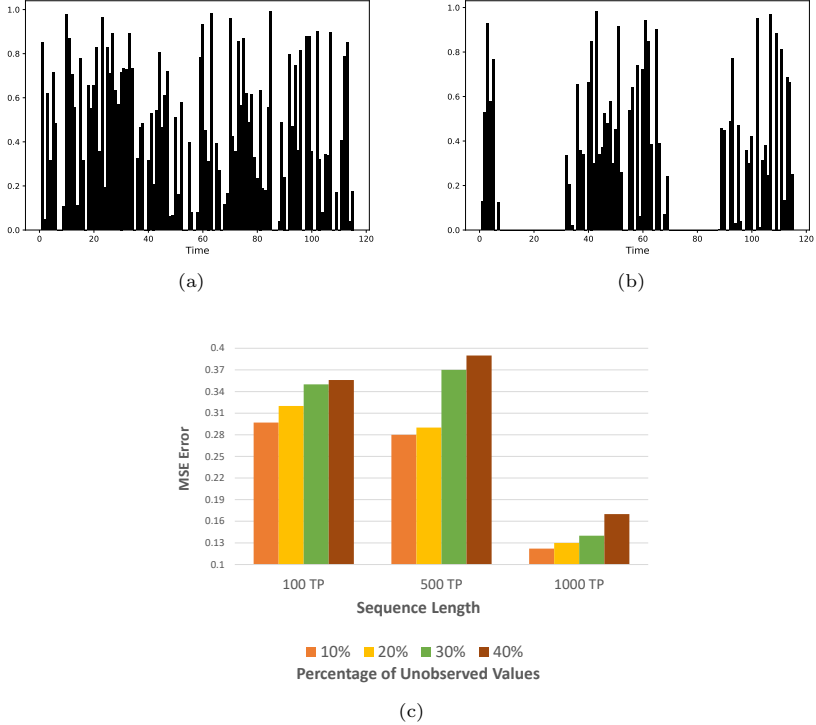


Fig. 1: (a) Bumpy irregular time series with short time lapses between observations. (b) Intermittent irregular time series with long time lapses between observations. (c) The performance of ODE-RNN on different sequence lengths (100, 500, and 1000 time points) with different amounts of unobserved values. The results show that ODE-RNN is affected by the length of the time lapse between observations.

non-linear relation between samples, (3) a customized ODE-RNN (Cross-level ODE-RNN) to model the irregular samples and provide a continuous effective representation for the sequences.

2 Motivation: ODE-RNN limitation

Irregular time series occur in many fields, particularly for medical systems where the data is captured when needed leading to gaps in the sequences. These gaps may sometimes extend to long periods, for example, if a patient misses his\her appointments or fails to use the medical devices at home regularly. Moreover, many observations will not be captured in systems and sensor failure situations, resulting in irregular and partially-observed time series. Figures 1.a and b show the difference between two types of irregular time series: (a) Bumpy series: irregular time series with less unobserved values (short time

lapse between observations (gaps), where the gaps are frequent and short. (b) Intermittent series: irregular time series with long gaps. This type occurs with more extended series and too many unobserved values for a long period [12]. Using these concepts, we analyze the behavior of the traditional ODE-RNN [9]. We conduct experiments on synthetic datasets (Described in Section 6.1) and study the model’s performance when having different lengths of sequence data with different amounts of unobserved values. Figure 1.c shows the baseline results of the traditional ODE-RNN model trained on sequence data of size 1000 samples and lengths of 100, 500, and 1000 time points. For each experiment, we used different percentages of consecutive missing observations (ranging from 10% to 40%).

The model shows the same pattern for different sequence lengths. The performance has an inverse relation with the number of unavailable observations. For example, when having 30% of unavailable data, the performance decreases by (17.8%, 32%, and 14%) on average compared with having 10% of unavailable values for sequence lengths 100, 500, and 1000 respectively. We intend to cut out points consecutively to address the effect of the time-lapse length (gap size) on the performance of the ODE-RNN model. Based on these results, we conclude that the ODE representation of continuous unobserved data may vary based on the amount of available data and the length of the sequences.

3 Problem and contribution statements

3.1 Problem statement

General Definition: we consider modeling N sporadically observed time series with D dimensions. For example, data from N samples (e.g. patients). Where D variables are potentially measured at a specific time point i . Each time series $TS \in (1, \dots, N)$ is measured at time points P_{TS} . Where P_{TS} is defined by a vector of observation times $i_{TS} \in \mathbb{R}^{P_{TS}}$. The values of the observations are defined by a value matrix $x_{TS} \in \mathbb{R}^{P_{TS} \times D}$ and mask matrix $m_{TS} \in (0, 1)$ that indicates if the variable is observed or not. We assume TS to be sporadically sampled when some samples x have m_{ts} equal to (0) at one or more time points. The goal is to effectively model the sporadic time series by finding the best continuous representation for the sequences.

3.2 Contribution statement

We demonstrate how ODE-based models may provide inaccurate and restricted hidden trajectories as they are affected by the length of the time lapse between observations. Therefore, we propose CrossPyramid network (Illustrated in Figure 2). In summary, CrossPyramid relies on a novel ODE AutoEncoder to learn the best representation of the data, followed by an attention module to categorize the learned representations based on the relations between samples. Finally, by defining the set of related representations for each sequence, a new ODE-RNN (Cross-level ODE-RNN) is designed and used to

model the time series by reaching all previously learned information. The main objective of CrossPyramid is to generalize the hidden state. In ODE-RNN the hidden state between observations is defined by the last observed value, making it very restrictive for the model to follow one initial value for a long time. We aim to find a representation that considers more available information based on the correlation between samples without blurring the original representation for the sequences. The final model has three key features: (1) Provides unrestricted ODE representation for the unobserved data by relying on different ODE-based hidden trajectories. (2) Learns the best representation of the sequences. (3) Maintains a good continuous representation over a long period. (4) Achieves state-of-the-art performance against other recent models for forecasting, re-generating, and classification tasks on multivariate and univariate datasets.

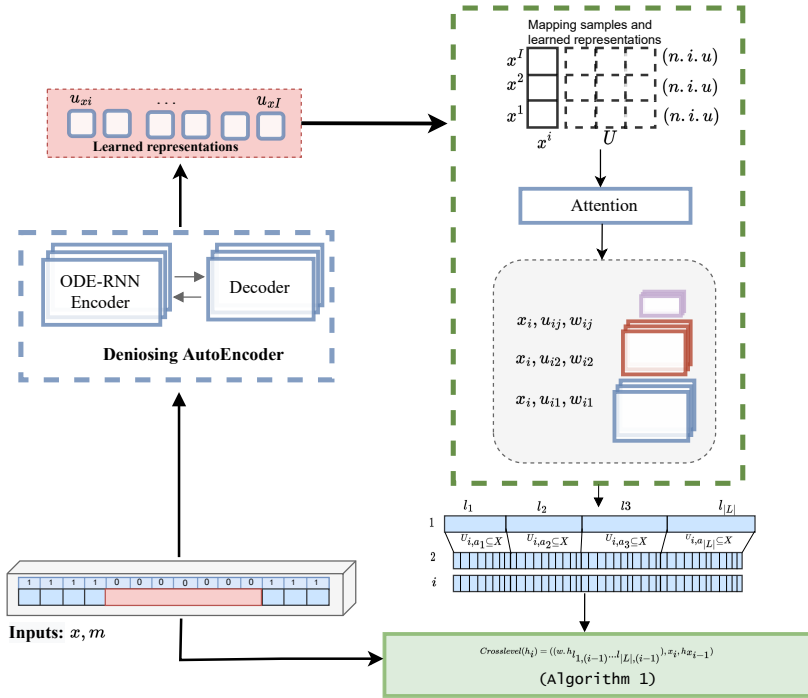


Fig. 2: The architecture of CrossPyramid model consists of AutoEncoder, Pyramid Attention, and Cross-level ODE-RNN. Where U : the best-learned representations, W : a set of importance weights. l : a level number from 1 to $|L|$, and i : the time point.

4 Background

Irregularity issues are related to the non-uniform interval between observations. In regular time series, the data follows a specific temporal sequence with a regular interval (For example, samples are always observed daily). While in irregular time series, samples are observed with unevenly spaced intervals. This issue is common for data captured from humans (such as medical data and human behavior data [13]), where the system depends on people’s commitment [2, 12, 14]. Also, it might be caused by capturing data from heterogeneous sources and sensors [15, 16]. However, irregular sampling is contrary to the machine learning models that assume fixed-size features [17]. Until the last few years, traditional techniques were used to handle irregularity, including analyzing fully-observed samples, performing a features analysis rather than a temporal analysis, or re-sampling and imputation [3, 12]. Nevertheless, these methods might destroy temporal information and dependencies.

RNN shows an outstanding performance in modeling temporal data; on the other hand, it assumes fixed laps between observations and fully observed samples. As appear in Equation 1, RNN defines a hidden state only when there are observations. At the same time, the hidden state between observations is static, which causes a weak performance when applying RNN to irregular sequences.

$$h_i = RNNCell(h_{i-1}, x_i) \quad (1)$$

To solve the issue, researchers proposed RNN decay which adds the time gap between observations into the hidden presentation. Also, they defined the hidden state h between observations using an exponential decay function toward zero. As shown in Equation 2 [18–20].

$$h_i = \begin{cases} RNNCell(h_{i-1}, \Delta t, x_i) & m_i = 1 \\ RNNCell(h_{i-1}, \exp\{\tau\Delta t\}, x_i) & m_i = 0 \end{cases} \quad (2)$$

Where τ is a decay rate parameter, Δt is the time gap between t_i and t_{i-1} and m_i is a mask value indicates if x_i is available or not. However, RNN decay’s performance was not different compared with the traditional RNN.

Recently, many effective models were established for irregular data after the development of the Neural Ordinary Differential Equations (Neural ODEs) [7] in 2018. Neural ODEs are a continuous-time model that defines a latent variable h_i as the solution to an ODE initial value. Rather than specifying a discrete sequence of hidden layers, a continuous representation became possible using the parameterization of the derivative as Equation 3 and 4.

$$\frac{dh(t)}{dt} = f\theta(h(t), t) \quad \text{where } h(t_0) = h_0 \quad (3)$$

$$h_0, \dots, h_n = \text{ODESolve}(f\theta, h_0, (t_0, \dots, t_n)) \quad (4)$$

To utilize this advantage of the hidden state in Neural-ODEs, recent models like ODE-RNN and Latent ODEs [9] have presented a continuous-time latent state, where the formation of the dynamics between observations is not predefined. These models define the state between observations to be the solution to an ODE, while normal RNN hidden cells (Equation 5) are used to update the hidden state at each observation. Therefore the trajectories of the hidden state between observations are defined by the last observed value.

$$h_i = \begin{cases} \text{RNNCell}(h_{i-1}, x_i) & m_i = 1 \\ \text{ODESolve}(f\theta, h_{i-1}, (t_{i-1}, \dots, t_i)) & m_i = 0 \end{cases} \quad (5)$$

As a particular case of the ODE-RNN model, Brouwer et al. provided GRU-ODE-Bayes [10], which includes a continuous-time version of the GRU (GRU-ODE) and Bayesian update network to handle the sporadic observations. The model combines GRU-ODE and GRU-Bayes. Where the first one is used to update the hidden state $h(i)$ in continuous time between the observations, the second part is responsible for transforming the hidden state based on the new observation from $h(i)$ to $h(i + 1)$.

Many recent DE-based models have been presented over the last couple of years [21–23], including Controlled Differential Equation (CDE) [22] and Neural RDE [23]. CDE is designed to overcome the challenge of modifying the hidden trajectories based on newly received data. Whereas ODE is defined by the initial state without a direct way to modify it, CDE updates the driven value of the ODE equation ds to be a matrix-vector dXs . Therefore the solution of CDE depends continuously on the evolution of x (driven by the control X). RDE model is an extended Neural CDE where the data is modeled without embedding the interpolated path to increase memory efficiency, especially for long sequences.

Other studies have been presented to model irregular time series by improving ODE models using attention [17, 24, 25] and LSTM [26]. Furthermore, ODE has recently been applied in various fields, as in [27], the authors studied the robustness of the Neural ODE model and proposed time-invariant steady neural ODE (TisODE). Their model was applied to the image classification task by removing the time dependence of the dynamics in an ODE [28].

However, in ODE-based models, numerical integration plays a significant role, and their behavior is still under investigation. Therefore, researchers have started investigating the robustness of differential equations. The authors in [29] tried to analyze the performance of the ODE-based models and explored the strength of different ODE architectures. In [30], the authors analyzed the relation between differential equations and ResNet. They showed that the ODE-based models have strong dependencies between the model and the numerical solver. Furthermore, many experiments were conducted in [31] to show how the numerical solver affects the model. The authors also offered a

convergence test to select the solver that makes the Neural ODEs learn good continuous dynamics.

5 Method

This article proposes an irregular time series modeling system that can yield generalized continuous hidden representations for unobserved values. As shown in Figure 2, the model consists of three main parts: (1) ODE Auto Encoder: learns the best-hidden representations using neural ODE. (2) Pyramidal attention method: defines the correlation between samples. (3) Cross-Level ODE-RNN: a generalized form of ODE-RNN to model partially-observed irregular time series.

5.1 ODE Auto-Encoder

Following the idea of Denoising Auto-Encoder (AE) [11] where a corrupted input is fed into the encoder with the task of obtaining a good embedding. Our ODE-based AE finds the optimal hidden representation (ODE hidden trajectory) that minimizes the reconstructing error between original data X and decoder output Y . The task is reconstructing X' (corrupted X) to the original data X . The proposed ODE AE is presented in Figure 3, and consists of the following steps:

- Generate x'_n by corrupting each observed x_n sample using a `cut_out` function based on a specific number of points to be removed from the timeline.
- Each corrupted x'_n is processed by ODE-RNN encoder to learn the hidden representation h_i at each time point i . As Equations (6) and (7).

$$h'_i = ODE_RNN(t_i) = ODEsolve(f\theta, h_{i-1}, (t_{i-1}, \dots, t_i)) \quad (6)$$

$$h_i = ODE_RNN(x_i) = RNNCell(h_{i-1}, x_i) \quad (7)$$

- The latent representations are solved back and decoded to the data space (undo the effect of a corruption process), where a decoder model of linear sequence layers generates a predicted data y_n .
- The generated data y_n is compared to the original x_n with the goal of minimising the re-generating error between y_n and x_n as $[arg_{\rho} min L(X, Y)]$. Where $\rho = \{W, W', b, b'\}$ are the parameter to be optimized for encoder and decoder, $L(\cdot)$ is the loss function to measure the similarity between X and Y .

5.2 Pyramidal attention

To generalize the ODE-RNN, we consider the latent representations of all samples to represent the unobserved values. We use the previously learned hidden states to define a set of latent representations for each sequence x_n based on the correlation between samples. As shown in Figure 2, we first map

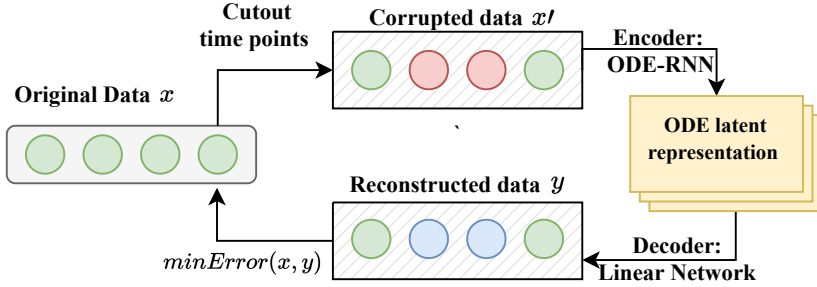


Fig. 3: Illustration of the proposed ODE AutoEncoder.

the original data (x) to the learned representations (u) by embedding both vectors as Equation 8 and 9. Where φ refers to the embedding layer and θ is learning weights.

$$e_x^{in} = \varphi_x(x_i^n, \theta_{\varphi_x}) \quad (8)$$

$$e_u^{in} = \varphi_u(u_i^n, \theta_{\varphi_u}) \quad (9)$$

Next, a concatenate layer combines both vectors followed by an attention layer that defines an attention score to find the importance rate α_{x_i} between each x and u using Softmax function as the following formula:

$$S_{x_{in}} = (e_x^{in} \oplus e_u^{in}) \cdot \theta_s \quad (10)$$

$$\alpha_{x_n} = \frac{\exp(S_{x_i})}{\sum_j \exp(S_{x_j})} \quad (11)$$

The assigned importance weights α for each sequence x_n are used to generate a set of hierarchical levels of related latent representations as $L = u_{1n}, u_{2n}, \dots, u_{in}$. At this stage, we use pyramidal sorting for each sample and corresponding learned representations (As shown in Algorithm (1)) according to the attention weight. The pyramid is generated by dividing the learned hidden representations into different levels. For example, the hidden representation with a higher importance rate for a specific sample is considered more related and added to the upper level of the pyramid. In contrast, the hidden representation with a lower importance rate is considered less related to that sample and added to the bottom level of the pyramid. Finally, representations at the upper level are given higher weights than representations at the bottom level. Sorting the learned representations based on the correlation for each sample has privileges over selecting one best-related representation, as it

allows consideration of information from all samples and reduces the risk of relying on one sample to represent the unobserved values for another sample.

Algorithm 1: Pyramidal sorting

Input: Importance rates ($Score(N * N)$), Learned_rep. ($u(N * L_D)$),
number_of_Level (L)

```

1 sortedUn = []
2 sortedU = []
3 for n in 1, 2, ..., N do:
4     sn = Score[n,]
5     for l in 1, 2, ..., L:
6         MeanV = mean(sn)
7         CL_sample = [sn <= MeanV].mean()
8         sn = [sn > Mean]
9         sortedUn.append(CL_sample)
10 end for
11 sortedU.append(sortedUn)

```

Output: sortedU

5.3 Cross-level ODE-RNN

Using the best learned hidden representations, we define a Cross-level ODE-RNN network (shown in Figure 4) that does not only consider the last observed value to generate a continuous representation for the unobserved part but also uses the learned ODE trajectories that were learned from different samples. The implementation of the Cross-level ODE-RNN is represented in Algorithm 2. ODESolver is used to define the hidden state at time $i + 1$ based on the last observed value (initial value), while another ODESolver is used to define a hidden state trajectory for $i + 1$ for other samples (ODESlover from the previously mentioned ODE AE). Finally, RNN cell is used to find the hidden state when there is an observation based on hidden states from ODESolver for the current sample, hidden states of other samples, and the current value of x_i . The ordinary differential equation is identified in the following form:

$$\frac{\partial h}{\partial x} = f_{\theta}(x_{t+T}, h_t, T) - \tau h \tag{12}$$

In other words, The hidden state will be defined based on the last hidden state and the current value of x_i for each x_i when $m_{x_i} = 1$ and it is defined based on the ODE solver for the last hidden state and the hidden states learned from other samples when $m_{x_i} = 0$. The previously learned state are combined and multiplied by a specific weight based on their level of correlation to the sample (generated by the previous module), As the following Equations (13,14,15):

$$L_{x_i} = \{l_1, l_2, \dots, l_L\} \tag{13}$$

$$\text{cross-level}(h_i + 1) = W.l_1, W.l_2, \dots, W.l_L \quad (14)$$

$$h_{i+1} = \text{RNNCell}(h_{i+1}, \text{cross-level}(h_i + 1), x_{i+1}) \quad (15)$$

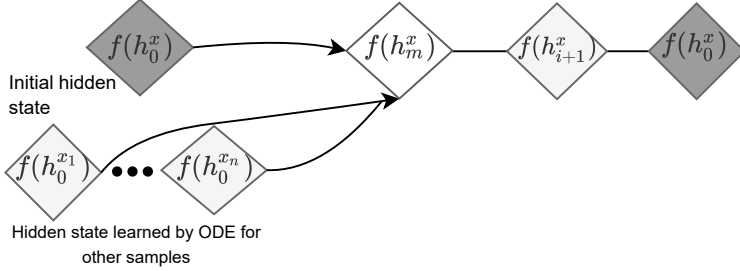


Fig. 4: The architecture of Cross-level ODE-RNN model (green part of Figure 2). Continuous-time modeling for irregular samples. Where h_0 is the initial state. $f(\cdot)$ is an ODE cell (update function) that use to solve ODE for h . $h_0^{x_n}$ is the previously learned trajectories from sample x_n at the same time point.

Algorithm 2: Cross-level ODE-RNN

Input: Data points X , timestamps I and missing-value mask M

1 $h_0 = 0$

for i **in** $1, 2, \dots, I$ **do:**

$\dot{h}_{i+1} = \text{ODESolve}(f_\theta, h_{x_i}, (t_i, t_{i+1}))$ // Solve ODE to get state at t_{i+1} based on last hidden state of x_i .

2 $\bar{h}_{i+1} = \text{ODESolve}(f_\theta, h_{X_i}, (t_i, t_{i+1}))$ // Solve ODE of h_i of other sample in X .

3 $h_{i+1} = \text{RNNCell}(\dot{h}_{i+1}, \bar{h}_{i+1}, x_{i+1})$

4 **end for**

Output: h_T

5 **Pass;**

To clearly show the difference between the traditional ODE-RNN and Cross-level ODE-RNN, Figure 5 shows the difference between hidden state trajectories for one sample using both models. The hidden state between observations for cross-level ODE-RNN is affected by other hidden states learned from other samples.

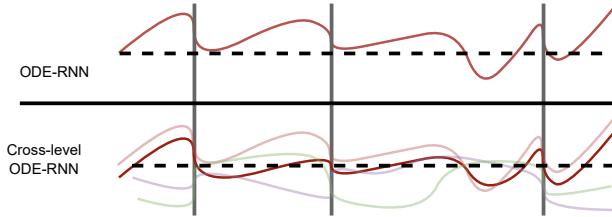


Fig. 5: Hidden state trajectories. Vertical lines show observation times. Horizontal lines show hidden states. The ODE-RNN model defines states between observations using an ODE and is updated at each observation time. Same for Cross-level ODE-RNN, but the states between observations are affected by other hidden states trajectories.

6 Experiments

6.1 Datasets

We use several datasets to evaluate our model: three synthetic datasets (Toy data), three benchmark real-world forecasting datasets, and one real-world classification dataset. The following list is a summary for each dataset:

- **Toy data:** We generate three synthetic data with 1000 samples of periodic trajectories. The Gaussian function is used for each data to generate sequences with different lengths. We refer to data with 100-time points as Toy_1, the data with 500-time points as Toy_2, and data with 1000-time points as Toy_3. For each dataset, we call a cut-out function to sub-sample the data and generate sporadic sequences. We generate four sets for each one with different percentages of unobserved values (10%, 20%, 30%, and 40%). The cut-off function removes the value by setting it to (0) in the value and mask tensors. In total, 12 synthetic trajectories data are used to report the performance of the baselines and our model. This data shows the effect of sequence length and the number of unobserved values on the performance of the models.
- **Electricity Consumption Load (ECL):** ECL is a public dataset that describes the electricity consumption (Kwh) of 321 clients. We use data from one year and ten sites. We generate sequences of 30 days lag and 1-day ahead prediction. Since ECL is regular time series, we perform a cut-out function on the samples. We cut out 30% of the time point randomly to generate sporadic series. In total, 3350 sequences are used. ECL dataset is available at (<https://archive.ics.uci.edu/ml/datasets/ElectricityLoadDiagrams20112014>).
- **Electricity Transformer Temperature (ETT):** ETT is multivariate time series that include two years of hourly data [32]. The data has six features used to predict the electrical transformers’ oil temperature based on load capacity. We used the available small dataset from 2016 and generated 2000 sequences of 24 hours lag length and one-hour ahead prediction. For ETT we also perform 30% cut-out to generate sporadic series.

- **Weather Data:** We use the weather data which is available at (<https://www.ncei.noaa.gov/data/local-climatological-data>). This data describes local climatological for U.S sites. It includes 11 climate features and the target value (wet-bulb). We build sequences of 7-day lag information using the hourly data and one-hour ahead prediction. We use 2000 sequences and perform 30% cut-outs to generate irregular samples.
- **Physionet dataset:** Irregular medical data, describe measurements for patients in ICU. Physionet includes 48 measurements, 37 features, and a binary target value for in-hospital mortality. For our experiments, we used data for 1000 patients. Following [9], we round up the time stamps to one minute to speed up the training process.

6.2 Experiments details

Baselines: As our architecture is built based on ODE-RNN, we select ODE-RNN as a major baseline. We also compare our models’ performance to Latent-ODE (as it is a popular outperformed model for irregularly-sampled time series), classical time-series models (RNN and RNN-VAE), and a novel Neural DEs model (CDE).

Setup: For all experiments, we apply a shuffled splitting into a training and testing set. 80% of the samples are used for training, while the testing set holds the remaining 20%. We re-scale (normalize) the features between (0,1) for each dataset. To generate sparse data for ECL, ETT, and weather datasets, we randomly cut out samples by setting the value to zero for the value and mask vectors. We cut 30% of the time points for each sample for all forecasting real-world datasets. Physionet is a sparse dataset; therefore, no cutout function is performed. For model hyperparameters, we follow [9] and choose the hyperparameters that yield the best performance for the original ODE-RNN. We run both baselines and CrossPyramid with the exact size of the hidden state, the number of layers, and units. For AutoEncoder we use ODE-RNN for the encoder and a shallow sequential network of one linear layer to decode the data to the data space and solve back the ODE. The fifth-order ”dopri5” solver from ”torchdiffeq” python package is used as the ODE Solver (The same one used in the traditional ODE-RNN model). The AutoEncoder model generates a latent representation vector with shape $(N * I * U)$ where N is the number of samples, I is the time points, and U is a learned latent representation for the variables. The Attention network is built with two inputs Inp_1 and Inp_2 . Inp_1 is the original data of shape (N, I, D) and Inp_2 is the learned states for the AutoEncoder. The final output for the Attention layer is a (N, N) matrix that represents a score of importance between every two samples. We use Mean Squared Error (MSE) to evaluate the performance for both re-generating and prediction tasks and the Area Under Curve (AUC) for the classification task.

Table 1: MSE values for CrossPyramid compared with several baselines on three Toy data sets (with different percentages of unobserved values) and three real-world forecasting datasets.

Dataset		RNN	RNN VAE	Latent ODE	CDE ¹	ODE-RNN	CrossPyramid
% of Unb. Pt.							
Toy_1	10%	1.127	7.535	8.390	6.998	0.297	0.280
	20%	1.231	7.783	8.356	8.143	0.319	0.297
	30%	1.097	7.345	8.425	8.732	0.349	0.318
	40%	5.099	7.21	8.404	9.180	0.356	0.307
Toy_2	10%	0.106	7.855	8.334	7.340	0.028	0.027
	20%	0.131	7.884	8.391	8.384	0.029	0.026
	30%	0.095	7.671	8.166	9.351	0.037	0.030
	40%	0.128	7.565	8.072	9.882	0.039	0.032
Toy_3	10%	0.048	7.992	8.230	7.882	0.012	0.012
	20%	0.054	7.901	8.209	8.245	0.013	0.011
	30%	0.040	7.872	8.289	10.300	0.014	0.012
	40%	0.052	7.731	8.094	10.000	0.017	0.015
ECL		0.520	3.400	0.620	3.181	0.500	0.480
ETT		0.212	0.374	0.202	0.408	0.230	0.199
Weather		0.735	11.724	0.783	-	0.660	0.657

¹Experiments of CDE model are conducted on one random seed and only for Toy datasets, ECL and ETT due to its poor efficiency on long gaps sequences; also, as compared to the baselines, CDE takes four times more time to complete 200 epochs.

Table 2: Classification results (AUC) for CrossPyramid compared with the baseline models for Physionet dataset.

Method.	Physionet
RNN	0.667
RNN VAE	0.518
Latent ODE	0.701
ODE-RNN	0.692
CrossPyramid	0.712

6.3 Model performance

Tables 1 and 2 present the results of CrossPyramid model against different baselines. Table 1 shows the MSE values for the re-generating and forecasting tasks, while Table 2 describes the AUC for the classification task on Physionet dataset. The results show the average of three runs based on several random seeds to initialize the model parameters. The best performance is highlighted in bold. Generally, our method outperforms the baselines for all synthetic and real-world datasets. The ODE-RNN model achieves the best performance among all the baselines for re-generating and forecasting tasks. At the same time, the structure of RNN-VAE, and Latent ODE fail to model these partially observed datasets. Although the CDE model was established to overcome a

similar issue in the Neural ODE model, it requires a longer processing time and fails to solve the re-generating and forecasting tasks. Regarding classification tasks, Table 2 shows that CrossPyramid has the highest accuracy among all classifiers for the Physionet data. In contrast, Latent ODE had the best performance among the baselines.

Furthermore, we can see that the average performance for ODE-RNN and CrossPyramid on the Toy datasets is enhanced for longer sequences. For instance, the average MSE value for Toy_1 using the ODE-RNN model is (0.33), while it improved by more than (89%) to be (0.033) for Toy_2 dataset and (0.014) for Toy_3 dataset. Also, the same case appears for CrossPyramid where the MSE value decreased by more than (90%) when using Toy_3 and Toy_2 datasets in place of Toy_1. Additionally, compared to the main baseline (ODE-RNN), CrossPyramid performs better for datasets with fewer available observations. For example, as shown in Figure 6, for Toy_1 dataset with 10% of unobserved values, the performance improved by (5.5%) when using CrossPyramid compared with ODE-RNN. In contrast, it improved by (14%) for 40% of unobserved values for the same dataset. This indicates that our methodology of defining hidden states between observations by considering data from different sequences helps to provide better representation, especially when the available observations are limited. Moreover, both methods perform better for longer sequence lengths. The evaluation shows that the performance does not rely only on the available and unavailable observations ratio. Whereas with 10% of unobserved values for the (1000) time-point sequence (Toy_3 dataset), there are (900) available observations to learn. However, we can see that with 10% unobserved values for Toy_2 and Toy_3 datasets, the performance of both models (CrossPyramid and ODE-RNN) is almost the same.

Following that deep analysis for datasets with different lengths, we can draw attention to the following termination; (1) The process of irregular sequence modeling is quite challenging for shorter sequences. (2) The representations' efficiency for irregular series does not rely on the percentage of unavailable observations, as the total number of available observations also impacts the performance. However, as we report the average MSE and AUC for three times runs, Table 3 includes the standard deviation error for each dataset.

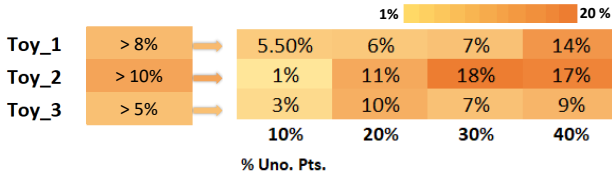


Fig. 6: The improvement percentage when using CrossPyramid over traditional ODE-RNN. The effect of our models increases for irregular sequences with longer time-lapses (gaps), especially when the sequence length is short.

Table 3: Test STD for three times run using CrossPyramid and several baselines for all datasets.

Dataset (% Uno.Pts.)		RNN	RNN-VAE	Latent ODE	ODE-RNN	CrossPyramid
Toy_1	10%	0.020526	0.002157	0.017776	0.000306	0.001
	20%	0.021234	0.058603	0.012023	0.001075	0.000577
	30%	0.019616	0.002121	0.009455	0.002246	0.000216
	40%	0.467988	0.002	0.011484	0.00017	2.83E-05
Toy_2	10%	0.00099	0.000707	0.005056	0.0012	0.000268
	20%	0.001669	0.000495	0.018031	0.00095	0.000212
	30%	0.001565	0.000431	0.006505	0.000699	0.000121
	40%	0.003536	0.000778	0.000283	0.00094	0.00012
Toy_3	10%	9.19E-05	7.07E-06	0.005774	0.000277	7.07E-06
	20%	7.07E-06	0.0007	0.000367	7.07E-07	8.77E-06
	30%	5.66E-06	0.000113	0.022528	6.5E-05	4.67E-05
	40%	7.07E-06	0.000778	0.000424	2.83E-06	8.7E-05
ECL	0.001762	0.004163	0.002379	7.92E-05	5E-05	
ETT	0.183313	0.005657	0.000356	0.008061	0.050871	
Weather	0.020785	0.221607	0.038891	0.027365	0.006518	
Physionet	0.014495	0.00360	0.00645	0.056569	0.006450	

7 Ablation study

To explore the effectiveness of CrossPyramid we apply a set of experiments to our model. We choose Toy datasets with 30% of unobserved values to analyze the performance of our method. As our main contribution is to consider more generalized latent trajectories to represent the unobserved data, we test the following different configurations to set up our model:

- Unified hidden trajectory: Use all learned representations without considering the relation between the samples (Removing the Attention module). Where all learned trajectories have the same uniform importance rate and will be combined by the average values of it.
- The most related trajectory: Use only the representations with the highest importance rate among all the learned representations.
- The least related trajectory: Use the representations with the least importance rates, where we can examine that the attention layer can generate accurate importance rates.

The results of the ablation study are presented in Table 4. The original CrossPyramid performance is superior to the other three configurations. On the other hand, using the most important latent representations outperforms the unified representation. The least important learned representations showed a weak performance, which indicates that the attention can learn the relations between samples. Moreover, as it is hard to justify the attention scores, we test additional architecture for CrossPyramid by replacing the attention layer with a deep clustering network. In this model, the data is clustered based on their

Table 4: The MSE results of the ablation studies on three Toy data sets and 30% unobserved values using three different configurations.

Config	Toy-1 2	Toy-2 3	Toy-3
Unified hidden trajectory	0.339	0.031	0.013
Most related trajectory	0.320	0.033	0.013
Least related trajectory	0.338	0.034	0.023
CrossPyramid	0.318	0.030	0.012

similarity. For each cluster, we get a unified ODE representation generated from samples belonging to that cluster and help to represent the unobserved values for the sample in the same cluster. Using the Toy_3 dataset with 30% of missing observation, the average MSE achieved was (0.033), which is better than traditional ODE-RNN but less effective compared with the attention network.

8 Model robustness

8.1 Case study

Two case studies are investigated in Figures 7 and 8 to further show the performance of the proposed method. The Figures show two samples from Toy_1 dataset, one with 10% of unobserved values, and the other has 40% of unobserved values. Each figure illustrates the sequence of the actual values, CrossPyramid predictions, and ODE-RNN predictions. We highlighted the predictions at different time points for more clarity. The generated sequences show that our model not only outperforms the overall sequences but also gives a higher prediction for the values that show up directly after the gap, even when the gaps are longer. In Figure 8, the difference between the predictions and the actual values at the time points (58 to 63) is about 8% less when using CrossPyramid compared with ODE-RNN. Moreover, more case studies are presented in Figure 9. Although the baseline is better at some time point (Figure 9.e), our proposed method outperforms most sequences. These cases implicitly prove that our model’s hidden representations for the unobserved time points are more related than the hidden state calculated in the traditional ODE-RNN.

8.2 Model interpretability

The total number of levels for the pyramid L (presented in Figure 2 and Section 5.2) is a very critical parameter in CrossPyramid. The value of L defines the height of the pyramid, hence the rates of importance that are given to each correlated sample. To research this parameter, we explore several pyramids with different sizes. Therefore, we used (1) Shorter pyramids with compacted

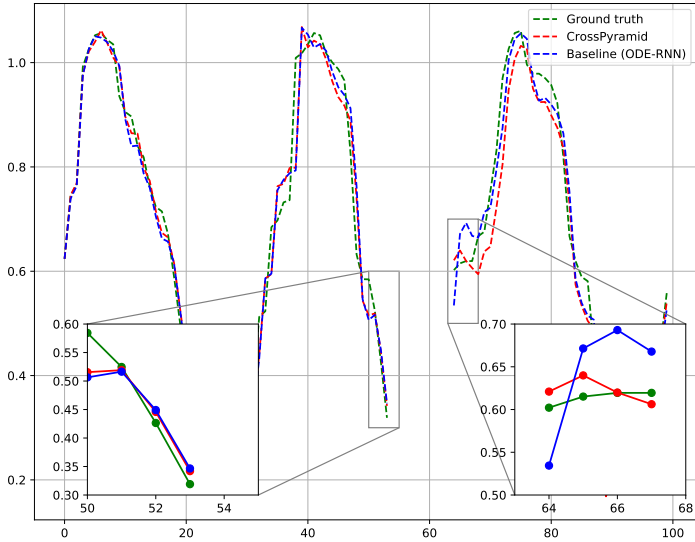


Fig. 7: Case Study 1: Sequences of one sample from Toy_1 datasets; with 10% unobserved values. Actual values are shown with the red dashed line, CrossPyramid predictions are shown with the green dashed line, and baseline (ODE-RNN) predictions are shown with the blue dashed line. CrossPyramid outperforms the baseline and can give more accurate predictions for the values that appear after the gap.

levels, which means few levels with more samples in each. (2) Higher pyramids with loose levels, meaning more levels but fewer samples in each. Figure 10 shows a heat map of the importance rates for samples from different datasets; each figure presents the top layer of the pyramid using different values of L . We found that very compacted layers mean giving more attention to less important samples as the radius between the samples and the correlated samples is long; hence less correlated samples will be considered more important. On the other hand, too loose levels mean focusing on very few correlated samples, which makes the model biased to a few samples.

9 Conclusion

In this work, we have proposed a novel ODE-based model to generalize hidden trajectories and analyze irregular data. We first explored the behavior of the traditional ODE-RNN model on partially observed sequences with several lengths and time lapses. Furthermore, we presented CrossPyramid model

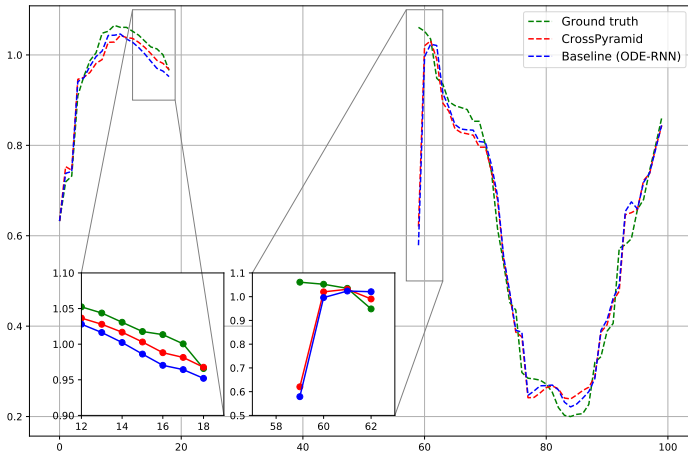


Fig. 8: Case Study 2: Sequences of one sample from Toy_1 datasets; with 40% unobserved values. Actual values are shown with the red dashed line, CrossPyramid predictions are shown with the green dashed line, and baseline (ODE-RNN) predictions are shown with the blue dashed line. CrossPyramid outperforms the baseline and can give more accurate predictions for the values that appear after the gap.

that can build unrestricted ODE representations for the unobserved values and maintain good continuous representations over a long period of time. Our model has three main parts: ODE AutoEncode that learns the representations of the data, an attention module to map the data with the learned representations based on the correlation between samples, and finally, cross-level ORE-RNN to model the data. Through extensive experiments, the results show that CrossPyramid outperforms other state-of-the-art models on different tasks and datasets. Our ablation study and case studies show that the framework of our model is able to improve the representation of the unobserved values for the partially-observed time series.

Acknowledgments. This research is supported by Australian Research Council (ARC) Discovery Project DP190101485.

References

- [1] Weerakody, P.B., Wong, K.W., Wang, G., Ela, W.: A review of irregular time series data handling with gated recurrent neural networks. *Neurocomputing* **441**, 161–178 (2021)

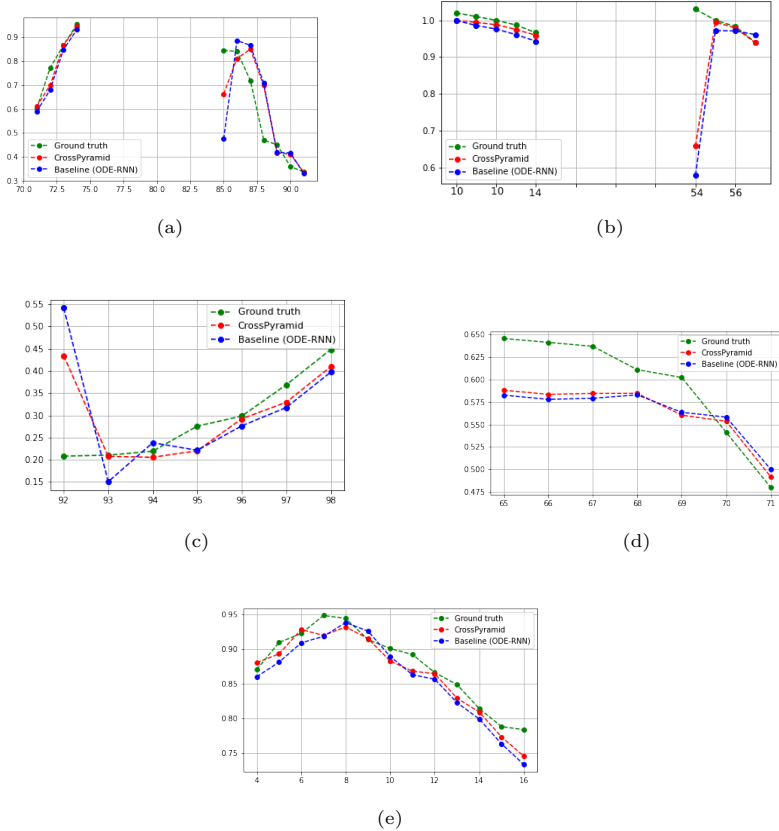


Fig. 9: Extra samples of the predictions generated by ODE-RNN and CrossPyramid.

- [2] Scargle, J.D.: Studies in astronomical time series analysis. ii-statistical aspects of spectral analysis of unevenly spaced data. *The Astrophysical Journal* **263**, 835–853 (1982)
- [3] Singh, B.P., Deznabi, I., Narasimhan, B., Kucharski, B., Uppaal, R., Josyula, A., Fiterau, M.: Multi-resolution networks for flexible irregular time series modeling (multi-fit). *arXiv preprint arXiv:1905.00125* (2019)
- [4] Kim, Y.-J., Chi, M.: Temporal belief memory: Imputing missing data during rnn training. In: *In Proceedings of the 27th International Joint Conference on Artificial Intelligence (IJCAI-2018)* (2018)
- [5] Ma, Q., Lee, W.-C., Fu, T.-Y., Gu, Y., Yu, G.: Midia: exploring denoising autoencoders for missing data imputation. *Data Mining and Knowledge Discovery* **34**(6), 1859–1897 (2020)

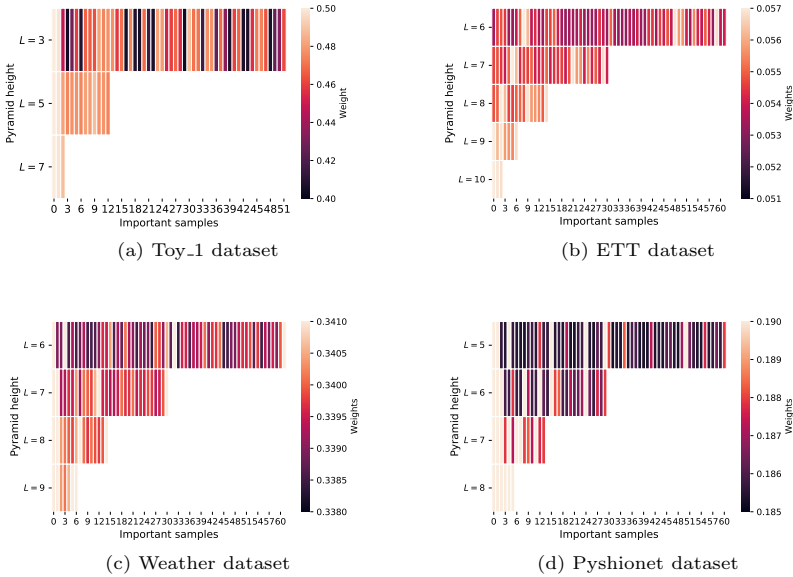


Fig. 10: Heat maps illustration of model behavior in terms of the attention weights for samples from different datasets using several values of L .

- [6] Khayati, M., Lerner, A., Tymchenko, Z., Cudré-Mauroux, P.: Mind the gap: an experimental evaluation of imputation of missing values techniques in time series. In: Proceedings of the VLDB Endowment, vol. 13, pp. 768–782 (2020)
- [7] Chen, R.T., Rubanova, Y., Bettencourt, J., Duvenaud, D.K.: Neural ordinary differential equations. Advances in neural information processing systems **31** (2018)
- [8] Sherstinsky, A.: Fundamentals of recurrent neural network (rnn) and long short-term memory (lstm) network. Physica D: Nonlinear Phenomena **404**, 132306 (2020)
- [9] Rubanova, Y., Chen, R.T., Duvenaud, D.K.: Latent ordinary differential equations for irregularly-sampled time series. Advances in neural information processing systems **32** (2019)
- [10] De Brouwer, E., Simm, J., Arany, A., Moreau, Y.: Gru-ode-bayes: Continuous modeling of sporadically-observed time series. Advances in neural information processing systems **32** (2019)
- [11] Vincent, P., Larochelle, H., Lajoie, I., Bengio, Y., Manzagol, P.-A., Botou, L.: Stacked denoising autoencoders: Learning useful representations

- in a deep network with a local denoising criterion. *Journal of machine learning research* **11**(12) (2010)
- [12] Zhang, C., Fanaee-T, H., Thoresen, M.: Feature extraction from unequal length heterogeneous ehr time series via dynamic time warping and tensor decomposition. *Data Mining and Knowledge Discovery* **35**(4), 1760–1784 (2021)
- [13] Deldari, S., Smith, D.V., Xue, H., Salim, F.D.: Time series change point detection with self-supervised contrastive predictive coding. In: *Proceedings of the Web Conference 2021*, pp. 3124–3135 (2021)
- [14] Lipton, Z.C., Kale, D., Wetzel, R.: Directly modeling missing data in sequences with rnns: Improved classification of clinical time series. In: *Machine Learning for Healthcare Conference*, pp. 253–270 (2016). PMLR
- [15] Deldari, S., Smith, D.V., Sadri, A., Salim, F.: Espresso: entropy and shape aware time-series segmentation for processing heterogeneous sensor data. *Proceedings of the ACM on Interactive, Mobile, Wearable and Ubiquitous Technologies* **4**(3), 1–24 (2020)
- [16] Abushaqra, F.M., Xue, H., Ren, Y., Salim, F.D.: Piets: Parallelised irregularity encoders for forecasting with heterogeneous time-series. In: *2021 IEEE International Conference on Data Mining (ICDM)*, pp. 976–981 (2021). IEEE
- [17] Shukla, S.N., Marlin, B.M.: Multi-time attention networks for irregularly sampled time series. *arXiv preprint arXiv:2101.10318* (2021)
- [18] Mozer, M.C., Kazakov, D., Lindsey, R.V.: Discrete event, continuous time rnns. *arXiv preprint arXiv:1710.04110* (2017)
- [19] Cao, W., Wang, D., Li, J., Zhou, H., Li, L., Li, Y.: Brits: Bidirectional recurrent imputation for time series. *Advances in neural information processing systems* **31** (2018)
- [20] Che, Z., Purushotham, S., Cho, K., Sontag, D., Liu, Y.: Recurrent neural networks for multivariate time series with missing values. *Scientific reports* **8**(1), 1–12 (2018)
- [21] Jia, J., Benson, A.R.: Neural jump stochastic differential equations. *Advances in Neural Information Processing Systems* **32** (2019)
- [22] Kidger, P., Morrill, J., Foster, J., Lyons, T.: Neural controlled differential equations for irregular time series. *Advances in Neural Information Processing Systems* **33**, 6696–6707 (2020)

- [23] Morrill, J., Salvi, C., Kidger, P., Foster, J.: Neural rough differential equations for long time series. In: International Conference on Machine Learning, pp. 7829–7838 (2021). PMLR
- [24] Jhin, S.Y., Lee, J., Jo, M., Kook, S., Jeon, J., Hyeong, J., Kim, J., Park, N.: Exit: Extrapolation and interpolation-based neural controlled differential equations for time-series classification and forecasting. arXiv e-prints, 2204 (2022)
- [25] Yuan, X., Jia, Z., Li, L., Wang, K., Ye, L., Wang, Y., Yang, C., Gui, W.: A sia-lstm based virtual metrology for quality variables in irregular sampled time sequence of industrial processes. *Chemical Engineering Science* **249**, 117299 (2022)
- [26] Lechner, M., Hasani, R.: Learning long-term dependencies in irregularly-sampled time series. arXiv preprint arXiv:2006.04418 (2020)
- [27] Yan, H., Du, J., Tan, V.Y., Feng, J.: On robustness of neural ordinary differential equations. arXiv preprint arXiv:1910.05513 (2019)
- [28] Garsdal, M., Sogaard, V., Sorensen, S.: Generative time series models using neural ode in variational autoencoders. arXiv preprint arXiv:2201.04630 (2022)
- [29] Habiba, M., Pearlmutter, B.A.: Neural ordinary differential equation based recurrent neural network model. In: 2020 31st Irish Signals and Systems Conference (ISSC), pp. 1–6 (2020). IEEE
- [30] Ott, K., Katiyar, P., Hennig, P., Tiemann, M.: Resnet after all: Neural odes and their numerical solution. In: International Conference on Learning Representations (2020)
- [31] Krishnapriyan, A.S., Queiruga, A.F., Erichson, N.B., Mahoney, M.W.: Learning continuous models for continuous physics. arXiv preprint arXiv:2202.08494 (2022)
- [32] Zhou, H., Zhang, S., Peng, J., Zhang, S., Li, J., Xiong, H., Zhang, W.: Informer: Beyond efficient transformer for long sequence time-series forecasting. In: Proceedings of AAAI (2021)